Fabrication of a Porphyrin-modified Reduced Graphene Oxide Electrode

Permsak Chairat and Patchanita Thamyongkit*

Department of Chemistry, Faculty of science, Chulalongkorn University, Bangkok, Thailand
*Corresponding author, E-mail: patchanita.v@chula.ac.th

Abstract

In this work, [5,10,15,20-tetra(2,2-bithiophen-5-yl)porphyrinato]Cobalt (Co-T2TP) was synthesized by a two-step procedure and ErGO/ITO-coated glasses were prepared and used as substrates for electropolymerization of Co-T2TP. Electrochemically reduced graphene oxide (ErGO) films on ITO-coated glasses were obtained from reduction of graphene oxide (GO) in 0.1 M Na_2SO_4 solution using cyclic voltammetry. Electrochemical study of the resulting ErGO/ITO-coated glass electrodes was performed by using ferrocene as a redox probe. Co-T2TP was successfully synthesized with 10% overall yield confirmed by NMR and mass spectrometry. 0.5 mM Co-T2TP was used as a monomer to electropolymerize on the ErGO/ITO-coated glass electrodes by mean of cyclic voltammetry in dichloromethane solution containing 0.1 M Tetrabutylammonium hexafluorophosphate (nBu$_4$NPF$_6$). Fourier transformed infrared (FTIR) and Raman spectroscopy and UV-visible spectrophotometry were used to confirm the presence of ErGO and poly(Co-T2TP) on the ITO-coated glass electrodes. In future work, poly(Co-T2TP)/ErGO-ITO electrode will be used as a compartment of photoactive supercapacitor and heterogeneous electrocatalytic system.

Keywords**:** *Cobalt(II)-porphyrin, Electropolymerization, Carbon-based electrode, Reduced graphene oxide*

1. Introduction

Porphyrin is a macrocyclic aromatic compound that consists of four pyrrole units and four bridging carbon atoms in a planar conformation with numerous advantageous properties, such as structural robustness, attractive absorption and emission properties and strong aromaticity (Tanaka & Osuka, 2015). In addition, the photo-physical and chemical properties of the porphyrins are tunable by adding various metals in the center of the ring and introducing substituents at meso positions of the porphyrin ring (Huang, Nakanishi & Berova, 2000). Therefore, the porphyrins have been utilized in many applications, such as dye-synthesized solar cells (Yang et al., 2014), supercapacitors (Gao et al.,2017), photoelectrocatalysts for O_2 (Day & Wamser, 2017) and CO_2 reduction (García et al., 2014).

An indium tin oxide (ITO)-coated glass is commonly used as a transparent electrode, which exhibits good conductivity and optical transparency (Lippens & Muehlfeld, 2014). However, it presents several major limitations, including low surface area, narrow negative potential window in water (Benck et al., 2014) and unstable interface between polymer and ITO-coated glass (Sharma, Andersson & Lewis, 2011). Therefore, the organic polymers usually peel off from the electrodes and electron transfer rates between the organic polymers and ITO-coated glass electrode surface was reduced (Zhang et al., 2015). In order to overcome these limitations, carbon-based materials become of interest a complementary material for ITO-coated glass electrode, the carbon-based materials such as, carbon nanotubes (CNT), graphene and reduced graphene oxide, offer good conductivity, large surface area and good electrons transfer between electrode surface and organic polymer and improve the stability of organic polymer (Mani et al., 2016).

Graphene is a one-atom thick planar sheet of sp^2-bonded carbon atoms, which are densely packed in a honeycomb crystal lattice (Shams, Zhang & Zhu, 2015). This unique nanostructure is suitable for many applications, such as batteries (Chiam et al., 2018), supercapacitors (Son et al., 2017), and hydrogen storage (Tozzini & Pellegrini, 2013). Graphene can be prepared by several approaches, such as exfoliation of graphite, chemical vapor deposition (CVD), epitaxial growth (Marrani et al., 2017). However, the facile, low cost and bulk production method is a chemical reduction of exfoliated graphite oxide (GO) by using graphite as an initial material. However, this method employs hazardous chemicals, hydrazine, as reductants (Shao et al., 2010). To overcome this drawback, an electrochemical reduction process that can be done in non-toxic aqueous solutions, such as NaCl, Na_2SO_4, Na_3PO_4, KNO_3 and KCl, was proposed (Zhang

et al., 2012). Typically, the electrochemical synthesis of graphene is carried out via two steps, starting from GO being assembled on the electrodes by dip-coating, drop-casting, or spray-coating and then being subjected to the electrochemical reduction to obtain the electrochemically reduced graphene oxide (ErGO)-modified electrode (Kheirmand & Eshghi, 2015). In this study, we reported a synthesis of Co(II)-porphyrin containing polymerizable *meso*-bithiophenyl groups and the polymerization on the ErGO-modified ITO-coated glass electrodefor using in the photoactive supercapacitor or photoelectrocatalyst in further studies.

2. Objectives

1. To synthesize and characterize Co(II)-porphyrin containing polymerizable meso-bithiophenyl groups
2. To fabricate and characterize ErGO-modified ITO-coated glass electrode from graphene oxide using the electrochemical reduction process
3. To prepare polymer films of the Co(II)-porphyrin on the ErGO-modified ITO-coated glass electrode

3. Materials and Methods

3.1 General

All chemicals were analytical grade, purchased from commercial sources and used as received unless noted otherwise. ^{1}H-NMR (400 MHz) spectra was recorded in $CDCl_3$. Chemical shifts (δ) are reported in parts per million (ppm). Mass spectra were obtained using matrix-assisted laser desorption ionization (MALDI) mass spectrometry with α-Cyano-4-hydroxycinnamid a α-CCA) as a matrix. Morphology and elemental analysis were studied using scanning electron microscope (SEM) and energy-dispersive x-ray spectroscopy (EDS) at a magnitude of 500. Absorption spectrum of target compounds in toluene and polymer films were measured under 300 to 800 nm at room temperature. Raman spectroscopy was operated by using 532 nm laser and Raman spectra of materials were recorded under Raman shift 500 to 3300 cm^{-1}. FTIR spectra of materials were recorded under wave number 600 to 3700 cm^{-1} with ATR mode.

3.2 Synthesis of tetra(2,2-bithiophen-5-yl)porphyrin (T2TP)

Following a previously published procedure (Lindsey et al., 1994), bithiophene carboxaldehyde (389 mg, 2.00 mmol) was dissolved in propionic acid (8 mL) in a seal tube. Then, pyrrole (0.142 mL, 2.00 mmol) was added and the reaction mixture was stirred at 130 ^oC for 1 hour. After cooling down to room temperature, methanol was added and the resulting precipitate was collected by filtration. Purification of this crude solid by a silica column (1.5% TEA in CH_2Cl_2) gave **T2TP** as a deep purple solid (75 mg, 15%). ^{1}H-NMR (δ) –2.61 (s, 2H), 7.12 (dd, *J* = 3.6, 5.2 Hz, 4H), 7.34 (dd, *J* = 0.8, 5.2 Hz, 4H), 7.42 (dd, *J* = 0.8, 3.6 Hz, 4H), 7.58 (d, *J* = 3.6 Hz, 4H), 7.80 (d, *J* = 3.6 Hz, 4H), 9.17 (s, 8H); MALDI-TOF-MS m/z (%): found, 967.049 (100) (M^+); calcd 966.023 (M^+; M = $C_{52}H_{30}N_4S_8$).

3.3 Synthesis of tetra(2,2-bithiophen-5-yl)porphyrinato Cobalt(II) (Co-T2TP)

Following a previously published procedure (Jiao et al., 2007), a solution of **T2TP** (75 mg, 0.078 mmol) in $CHCl_3$ (25 mL) was metallated with a solution of $Co(OAc)_2{\cdot}4H_2O$ (97 mg, 0.39 mmol) in methanol (3 mL) under reflux for 2 hours. After removal of the solvent, the reaction mixture was redissolved in CH_2Cl_2 (50 mL), washed with water (50 mL), dried over anhydrous Na_2SO_4, and concentrated to dryness, and the resulting crude was purified by a silica column (1.5% TEA in CH_2Cl_2), followed by washing with hexanes to give **Co-T2TP** as a purple solid (mg, 65%). MALDI-TOF-MS m/z (%): found, 1022.729 (100) [M^+]; calcd 1022.941 (M^+; M = $C_{52}H_{28}N_4S_8Co$); UV–vis: λ_{abs} 449, 562, 607 nm.

3.4 Preparation of the ErGO-modified ITO-coated glass

A GO solution in Milli-Q water (0.125 mg/mL, 200 µL) was dropped on ITO-coated glass and dried at room temperature to obtain the GO film on the ITO-coated glass. After that, the GO film was

reduced by electrochemical reduction in a 0.1 M Na_2SO_4 aqueous solution under deoxygenated condition by means of cyclic voltammetry in a three-electrode one-compartment system using a GO/ITO-coated glass electrode as a working electrode (WE. A Pt plate and silver chloride coated on a silver wire (Ag/AgCl) were used as a counter electrode (CE) and a quasi-reference electrode (QRE) at a potential range of 0.3 V to – 1.4 V vs. Ag/AgCl (QRE) and a scan rate of 50 $mV \cdot s^{-1}$ for 10 cycles.

3.5 Electropolymerization of Co-T2TP

Electropolymerization of **Co-T2TP** was performed by the cyclic voltammetry in CH_2Cl_2 containing 0.5 mM **Co-T2TP** and 0.1 M nBu$_4$NPF$_6$ in a three-electrode one-compartment system using an ITO-coated glass or ErGO/ITO-coated glass electrode as a working electrode. Polymerization was electrochemically carried out under N_2 atmosphere at a potential ranging from 0 V to 1.4 V vs. Ag/AgCl (QRE) with a scan rate of 50 $mV \cdot s^{-1}$ and the number of scanning cycles of 10.

4. Results and Discussion

4.1 Synthesis and characterization

As shown in Scheme 1, the synthesis of the target compounds started from condensation between pyrrole and bithiophene carboxaldehyde under acid catalysis and subsequent oxidation by oxygen in air (Lindsey et al., 1994) to obtain the **T2TP**. ^{1}H-NMR spectra of **T2TP** exhibited signals of β-pyrrolic protons at 9.17 ppm, thienyl protons at 7.1 to 7.80 ppm and inner protons at −2.61 ppm. MALDI-TOF-MS found a molecular ion peak at m/z 967.049, which was consistent with the data reported by Keawsongsaeng et al. (2016) report, confirming that **T2TP** was successfully synthesized. After that the **T2TP** was subjected to cobalt-metalation using a method described by Jiao et al. (2007) to obtain **Co-T2TP**. Due to the paramagnetic property of Co(II) in **Co-T2TP**, the target compound was not characterized by ^{1}H-NMR. However, the MALDI-TOF-MS found a molecular ion peak at m/z 1022.729, suggesting that **Co-T2TP** could be synthesized by these two-step procedures with 10% overall yield.

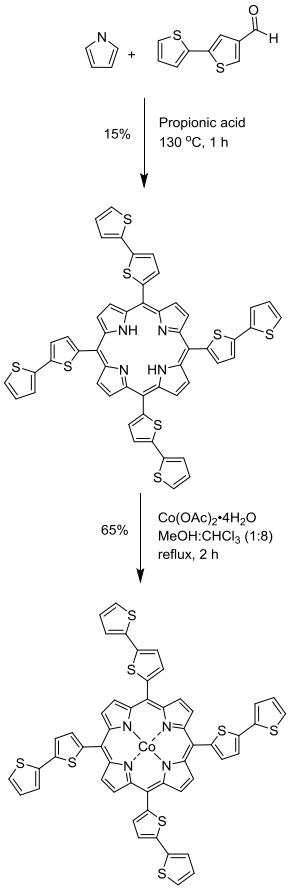

Scheme 1 Synthesis of **Co-T2TP**

4.2 Preparation of the ErGO-modified ITO-coated glass

Cyclic voltammograms for the electrochemical reduction of the drop casted GO film on the ITO-coated glass showed reduction potential onset at −1.2 V vs Ag/AgCl (QRE) with drastic current increase when the potential reached −1.4 V vs Ag/AgCl (QRE), which corresponded to the reduction of oxygen functional groups at the GO surface (Devadas et al., 2014). However, with the increasing number of scans, the GO reduction current was found to decrease, suggesting that the reduction of surface-oxygenated species at GO occurred quickly and irreversibly (Guo et al., 2009). These indicated that the GO was reduced to ErGO under this electrochemical reduction condition.

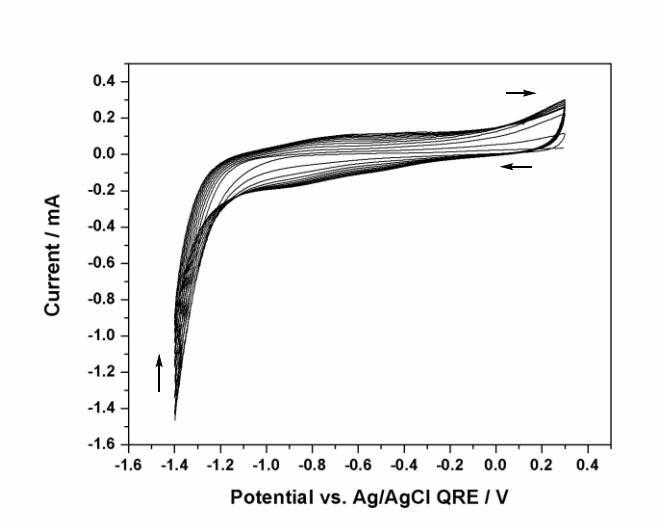

Figure 1 Cyclic voltammograms of the electrochemical reduction of the GO film on the ITO-coated glass

The morphology of the resulting ErGO films on the ITO-coated glasses was characterized by SEM as shown in Figure 2a, as the ErGO film revealed a wrinkled texture and well covered on ITO-coated glass surface which was agreeable with the EDS elemental mapping as shown in figure 2b. This EDS map illustrates the good distribution of ErGO on ITO-coated glass.

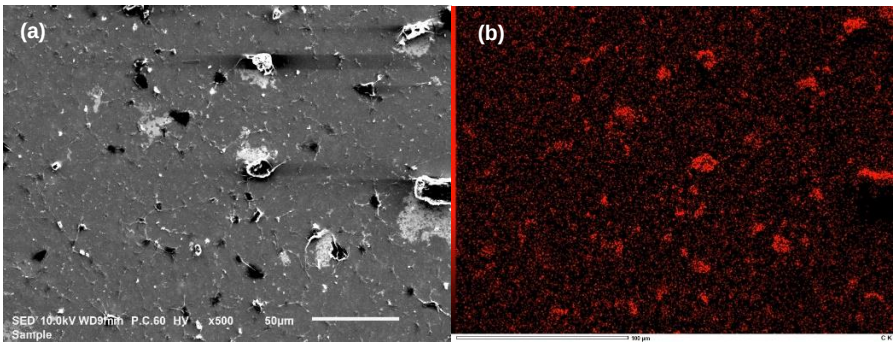

Figure 2 (a) SEM image and (b) EDS map of carbon element of ErGO film on ITO-coated glass

The original GO and resulting ErGO film on the ITO-coated glass was characterized by UV-visible spectrophotometry as shown in Figure 3. The maximum absorption of GO on the ITO-coated glass was observed at 386 nm, while that of the ErGO film on the ITO-coated glass was found at 393 nm. The redshift is attributed to rearrangement of electronic conjugation in the aromatic structure and confirmed that the oxygen functionalities in GO were reduced by the electrochemical method (Mutyala & Mathiyarasu, 2016).

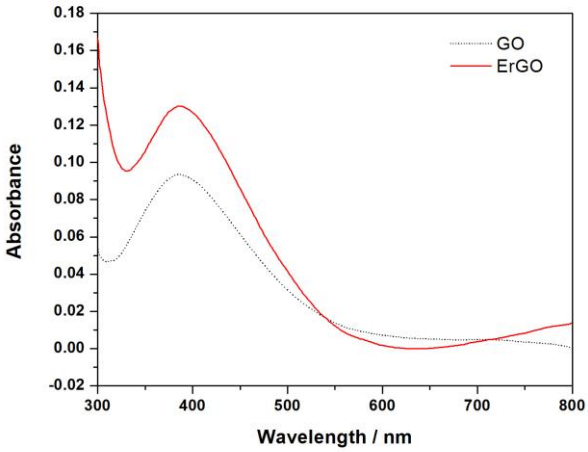

Figure 3 UV-visible absorption spectra of the GO and ErGO films on the ITO-coated glasses

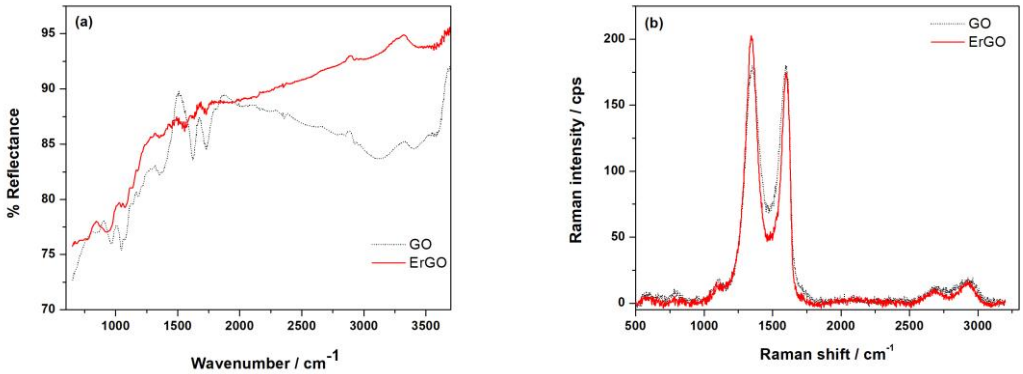

Figure 4 (a) FTIR and (b) Raman spectra of the GO (black dashed line) and ErGO films (red solid line) on the ITO-coated glass and ErGO

As shown in Figure 4a, FTIR spectrum of the pristine GO showed O-H stretching of carboxyl groups as a broad peak at 3383 cm^{-1}, C=O stretching at 1732 cm^{-1}, C=C stretching at 1621 cm^{-1}, O-H bending at 1351 $cm^{-1}$and C-O stretching of epoxy groups at 1046 cm^{-1}. In the case of ErGO, its FTIR spectrum showed very low intensity of OH-stretching at 3383 cm^{-1} and C=O stretching at 1732 cm^{-1}, indicating the reduction of GO under this electrochemical condition.

Figure 4b shows a Raman spectrum of the pristine GO film showed D and G peaks at Raman shift of 1350, 1598 cm^{-1}, respectively (Mekassa et al., 2017). The G band corresponds to in-plane bond stretching of the sp^2-carbon, whereas the D band is associated with various types of defects, such as vacancy-like defects, grain boundary edges, domain boundaries and electron doping (Alonso et al., 2017). In the case of the ErGO film, the D band shifted to 1343 with higher intensity than that of GO and D band was observed at 1598 cm^{-1} which similar to GO. The intensity ratio of the D to G bands (I_D/I_G) for the GO and ErGO films are 1.43 and 1.66, respectively. The higher I_D/I_G indicated the restoration of sp^2 carbon and decreased in the average sizes of sp^2 domains upon the reduction. Higher intensity in D band also suggested that more isolated graphene domains were presented in rGO as compared to GO and also indicated removal of oxygen moieties from GO after the reduction (Hidayah et al.,2017).

4.5 Electropolymerization of Co-T2TP

The electrochemical polymerization of **Co-T2TP** was performed using the ErGO-modified ITO-coated glass as the working electrode. In the case of using ErGO/ITO-coated glass as working electrode, the cyclic voltammogram exhibited three oxidation peaks at 0.75, 1 and 1.4 V vs. Ag/AgCl QRE (Figure 5). The first two peaks were consistent with the oxidation processed of the porphyrin ring and the last one corresponded to the oxidation of the *meso*-bithiophenyl groups (Shimidzu et al., 1995). With the increasing number of scans, the peak current of all three oxidation peaks current was found to increase. This behavior is attributed to the growth of polymeric film (San Martín et al., 2007).

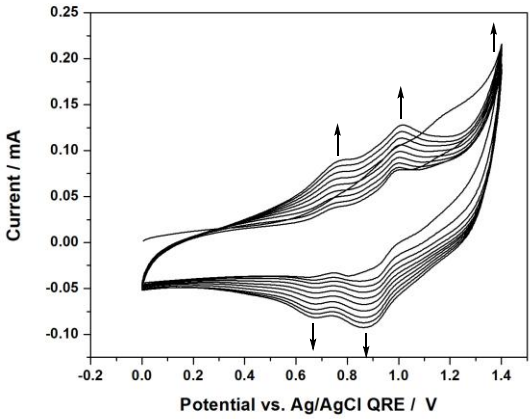

Figure 5 Cyclic voltammograms of the electropolymerization of **Co-T2TP** on the ErGO-modified ITO-coated glass

To confirm the presence of the Co(II)-porphyrin units in the resulting film that could imply the successful formation of the polymer of **Co-T2TP** (**poly(Co-T2TP)**), the absorption of the resulting film was investigated in comparison to that of Co-T2TP as shown in Figure 5. The results showed that the spectrum of **Co-T2TP** exhibited a characteristic intense Soret band at 449 and weak Q-bands at 562 and 607 nm. This absorption pattern was also observed for its polymer film with a broader feature slight red shift due to an extended π-conjugation system and possible macrocyclic aggregation in the polymer chains. Therefore, it can be concluded that the polymerization of **Co-T2TP** was achieved.

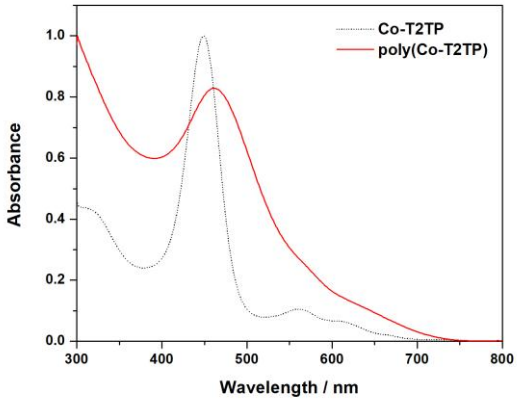

Figure 5 Normalized absorption spectra of a **Co-T2TP** solution in toluene (black dashed line) and the **poly(Co-T2TP)** film on the ErGO-modified/ITO-coated glass (red solid line)

5. Conclusion

The target porphyrin bearing the bithiophenyl *meso*-substituents was successfully synthesized by two-step processes in 10% overall yield. A transparent carbon-based electrode was successfully fabricated by electrochemical reduction of the dropcasted GO film on the ITO-coated glass and used on the working electrode for the electropolymerization of the target compound. Characterization by UV-visble spectrophotometry confirmed the formation of the ErGO film and the corresponding porphyrin polymer on the ErGO film. This electrode will be further studied for the photoactive supercapacitor and photoelectrocatalyst applications.

6. Acknowledgement

We gratefully acknowledge the financial support of the research from the Development and Promotion of Science and Technology Talents Project (DPST).

7. References

Alonso, R. M., San-Martín, M. I., Sotres, A., & Escapa, A. (2017). Graphene oxide electrodeposited electrode enhances start-up and selective enrichment of exoelectrogens in bioelectrochemical systems. *Scientific Reports*, *7*(1), 13726.

Benck, J. D., Pinaud, B. A., Gorlin, Y., & Jaramillo, T. F. (2014). Substrate selection for fundamental studies of electrocatalysts and photoelectrodes: inert potential windows in acidic, neutral, and basic electrolyte. *PloS One*, *9*(10), e107942.

Chiam, S. L., Lim, H. N., Hafiz, S. M., Pandikumar, A., & Huang, N. M. (2018). Electrochemical performance of supercapacitor with stacked copper foils coated with graphene nanoplatelets. *Scientific reports*, *8*(1), 3093.

Devadas, B., Madhu, R., Chen, S. M., & Yeh, H. T. (2014). Controlled electrochemical synthesis of new rare earth metal lutetium hexacyanoferrate on reduced graphene oxide and its application as a salicylic acid sensor. *Journal of Materials Chemistry B*, *2*(43), 7515-7523.

Day, N. U., & Wamser, C. C. (2017). Poly-tetrakis-5, 10, 15, 20-(4-aminophenyl) porphyrin films as two-electron oxygen reduction photoelectrocatalysts for the production of H2O2. *The Journal of Physical Chemistry C*, *121*(21), 11076-11082.

Gao, P., Chen, Z., Zhao-Karger, Z., Mueller, J. E., Jung, C., Klyatskaya, S., & Ruben, M. (2017). A porphyrin complex as a self-conditioned electrode material for high-performance energy storage. *Angewandte Chemie International Edition*, *56*(35), 10341-10346.

García, M., Aguirre, M. J., Canzi, G., Kubiak, C. P., Ohlbaum, M., & Isaacs, M. (2014). Electro and photoelectrochemical reduction of carbon dioxide on multimetallic porphyrins/polyoxotungstate modified electrodes. *Electrochimica Acta*, *115*, 146-154.

Guo, H. L., Wang, X. F., Qian, Q. Y., Wang, F. B., & Xia, X. H. (2009). A green approach to the synthesis of graphene nanosheets. *ACS nano*, *3*(9), 2653-2659.

Hidayah, N. M. S., Liu, W. W., Lai, C. W., Noriman, N. Z., Khe, C. S., Hashim, U., & Lee, H. C. (2017, October). Comparison on graphite, graphene oxide and reduced graphene oxide: Synthesis and characterization. In AIP Conference Proceedings (Vol. 1892, No. 1, p. 150002). AIP Publishing.

Huang, X., Nakanishi, K., & Berova, N. (2000). Porphyrins and metalloporphyrins: versatile circular dichroic reporter groups for structural studies. *Chirality: The Pharmacological, Biological, and Chemical Consequences of Molecular Asymmetry*, *12*(4), 237-255.

Jiao, J., Thamyongkit, P., Schmidt, I., Lindsey, J. S., & Bocian, D. F. (2007). Characterization of porphyrin surface orientation in monolayers on Au (111) and Si (100) using spectroscopically labeled molecules. *The Journal of Physical Chemistry C*, *111*(34), 12693-12704.

Keawsongsaeng, W., Gasiorowski, J., Denk, P., Oppelt, K., Apaydin, D. H., Rojanathanes, R., & Thamyongkit, P. (2016). Systematic investigation of porphyrin-thiophene conjugates for ternary bulk heterojunction solar cells. *Advanced Energy Materials*, *6*(20), 1600957.

Kheirmand, M., & Eshghi, A. (2015). Electrodeposition of platinum nanoparticles on reduced graphene oxide as an efficient catalyst for oxygen reduction reaction. *Iranian Journal of Hydrogen & Fuel Cell*, *2*(1), 7-12.

Lindsey, J. S., MacCrum, K. A., Tyhonas, J. S., & Chuang, Y. Y. (1994). Investigation of a synthesis of meso-porphyrins employing high concentration conditions and an electron transport chain for aerobic oxidation. *The Journal of Organic Chemistry*, *59*(3), 579-587.

Lippens, P., & Muehlfeld, U. (2014). *Indium tin oxide (ITO): Sputter deposition processes*. Handbook of Visual Display Technology, 1-16.

Mani, V., Huang, S. T., Devasenathipathy, R., & Yang, T. C. (2016). Electropolymerization of cobalt tetraamino-phthalocyanine at reduced graphene oxide for electrochemical determination of cysteine and hydrazine. *RSC Advances*, *6*(44), 38463-38469.

Marrani, A. G., Zanoni, R., Schrebler, R., & Dalchiele, E. A. (2017). Toward graphene/silicon interface via controlled electrochemical reduction of graphene oxide. *The Journal of Physical Chemistry C*, *121*(10), 5675-5683.

Mekassa, B., Tessema, M., Chandravanshi, B. S., Baker, P. G., & Muya, F. N. (2017). Sensitive electrochemical determination of epinephrine at poly (L-aspartic acid)/electro-chemically reduced graphene oxide modified electrode by square wave voltammetry in pharmaceutics. *Journal of Electroanalytical Chemistry*, *807*, 145-153.

Mutyala, S., & Mathiyarasu, J. (2016). A reagentless non-enzymatic hydrogen peroxide sensor presented using electrochemically reduced graphene oxide modified glassy carbon electrode. *Materials Science and Engineering: C*, *69*, 398-406.

San Martín, C., Dreyse, P., García, C., Calfumán, K., Villagra, D., & Isaacs, M. (2007). Electrochemical reduction of nitrite at polymeric Co (II)-tetra-3-amino-phenyl-porphyrin modified electrode. *Journal of the Chilean Chemical Society*, *52*(4), 1305-1308.

Shams, S. S., Zhang, R., & Zhu, J. (2015). Graphene synthesis: a Review. *Materials Science-Poland*, *33*(3), 566-578.

Shao, Y., Wang, J., Engelhard, M., Wang, C., & Lin, Y. (2010). Facile and controllable electrochemical reduction of graphene oxide and its applications. *Journal of Materials Chemistry*, *20*(4), 743-748.

Sharma, A., Andersson, G., & Lewis, D. A. (2011). Role of humidity on indium and tin migration in organic photovoltaic devices. *Physical Chemistry Chemical Physics*, *13*(10), 4381-4387.

Shimidzu, T., Segawa, H., Wu, F., & Nakayama, N. (1995). Approaches to conducting polymer devices with nanostructures: photoelectrochemical function of one-dimensional and two-dimensional porphyrin polymers with oligothienyl molecular wire. *Journal of Photochemistry and Photobiology A: Chemistry*, *92*(1-2), 121-127.

Son, I. H., Park, J. H., Park, S., Park, K., Han, S., Shin, J., & Choi, J. W. (2017). Graphene balls for lithium rechargeable batteries with fast charging and high volumetric energy densities. *Nature Communications*, *8*(1), 1561.

Tanaka, T., & Osuka, A. (2015). Conjugated porphyrin arrays: synthesis, properties and applications for functional materials. *Chemical Society Reviews*, *44*(4), 943-969.

Tozzini, V., & Pellegrini, V. (2013). Prospects for hydrogen storage in graphene. *Physical Chemistry Chemical Physics*, *1*5(1), 80-89.

Yang, G., Tang, Y., Li, X., Ågren, H., & Xie, Y. (2017). Efficient solar cells based on porphyrin dyes with flexible chains attached to the auxiliary benzothiadiazole acceptor: suppression of dye aggregation and the effect of distortion. *ACS applied materials & interfaces*, *9*(42), 36875-36885.

Zhang, H., Zhang, Y., Gu, C., & Ma, Y. (2015). Electropolymerized conjugated microporous poly (zinc-porphyrin) films as potential electrode materials in supercapacitors. *Advanced Energy Materials*, *5*(10), 1402175.

Zhang, X., Zhang, D., Chen, Y., Sun, X., & Ma, Y. (2012). Electrochemical reduction of graphene oxide films: Preparation, characterization and their electrochemical properties. *Chinese science bulletin*, *57*(23), 3045-3050.